The Scientific World Journal
Volume 2012, Article ID 149670, 5 pages
doi:10.1100/2012/149670

The ScientificWorldJOURNAL

Research Article

Thermoelectric Properties of $Ca_{1-x}Gd_xMnO_{3-\delta}$ (0.00, 0.02, and 0.05) Systems

Ankam Bhaskar, Chia-Jyi Liu, and J. J. Yuan

Department of Physics, National Changhua University of Education, Changhua 500, Taiwan

Correspondence should be addressed to Chia-Jyi Liu, liucj@cc.ncue.edu.tw

Received 12 June 2012; Accepted 5 August 2012

Academic Editors: M. Aksan, F. Aliev, and L. Koroleva

Polycrystalline samples of $Ca_{1-x}Gd_xMnO_{3-\delta}$ ($x = 0.00$, 0.02, and 0.05) have been studied by X-ray diffraction (XRD), electrical resistivity (ρ), thermoelectric power (S), and thermal conductivity (κ). All the samples were single phase with an orthorhombic structure. The Seebeck coefficient of all the samples was negative, indicating that the predominant carriers are electrons over the entire temperature range. The iodometric titration measurements indicate that the electrical resistivity of $Ca_{1-x}Gd_xMnO_{3-\delta}$ correlated well with the average valence of Mn^{v+} and oxygen deficiency. Among the doped samples, $Ca_{0.98}Gd_{0.02}MnO_{3-\delta}$ had the highest dimensionless figure of merit 0.018 at 300 K, representing an improvement of about 125% with respect to the undoped $GaMnO_{3-\delta}$ sample at the same temperature.

1. Introduction

Thermoelectric generators can convert waste heat into electric energy without using moving parts and without producing carbon dioxide gas, toxic substances, or other emissions. It is expected that thermoelectric power generation can provide a new energy source from the conversion of waste heat emitted by automobiles, factories, and other similar sources. For this purpose, oxide materials are potential candidates for a wide range of high-temperature applications due to their high chemical stability and the absence of harmful elements in their compositions. Since the discovery of large thermoelectricity in Na_xCoO_2 [1], enthusiastic efforts have been devoted to explore new oxides exhibiting high thermoelectric performances, and some layered cobaltites such as $[Ca_2CoO_3][CoO_2]_{1.62}$ and $[Bi_{0.87}SrO_2]_2[CoO_2]_{1.82}$ are found to exhibit interesting thermoelectric properties [2–4]. These p-type materials present large thermopower (>100 μV/K at 300 K), a relatively low electrical resistivity (~1–10 mΩ–cm at 300 K), and are expected to be incorporated in thermoelectric modules. More recently, theoretical predictions lead interest to focus on low-dimensional materials with a ZT of 2.4 in Nb-doped $SrTiO_3$ thin films due to the giant Seeback coefficient in the superlattices [5]. On the other hand, the intensive investigations on n-type oxides are still going on because their lower performances compared to p-type materials. Among these n-type materials, the perovskite $CaMnO_3$-based compound has been intensively studied due to its relatively low electrical resistivity and high Seebeck coefficient [6–10]. The decrease in the electrical resistivity by the means of cationic substitutions in the "A" site, like in $R_{1-x}A_xMnO_3$ [8] (R: rare earth cation, A: divalent cation such as Ca, Sr, Ba, and Pb), $La_{1-x}Sr_xMnO_3$ [9], $Ca_{1-x}Dy_xMnO_{2.89}$ [11], and $Ca_{1-x}La_xMnO_3$ [12]. Tang et al. [13] reported that Gd substitution of $Ca_{3-x}Gd_xCo_4O_{9+\delta}$ improved the figure of merit, which was about one order of magnitude larger than that of $Ca_3Co_4O_{9+\delta}$.

In these studies, we report thermoelectric properties of $Ca_{1-x}Gd_xMnO_{3-\delta}$ (0.00, 0.02, and 0.05) systems.

2. Experimental Details

Polycrystalline samples of $Ca_{1-x}Gd_xMnO_{3-\delta}$ (0.00, 0.02, and 0.05) were synthesized by the solid-state reaction from $CaCO_3$, Mn_2O_3, and Gd_2O_3 powders. The powders were heated at 1173 K for 10 h and at 1473 K for 20 h in air with intermediate grinding. The resulting powders were then pressed into parallelepiped and sintered in air at

1473 K for 20 h. The phase purity of resulting powders was examined by a Shimadzu XRD-6000 powder X-ray diffractometer equipped with Fe $K\alpha$ radiation. Electrical resistance measurements were carried out using standard four-probe techniques. Thermopower measurements were performed between 300 and 700 K using a steady-state technique with a temperature gradient of 0.5–2 K across the sample. A type E differential thermocouple was used to measure the temperature difference between the hot and cold ends of the sample, which was measured using Keithley 2000 multimeter [14]. The temperature difference was typically between 0.5 and 1 K. The thermopower of the sample was obtained by subtracting the thermopower of Cu Seebeck probes. Thermal conductivity measurement was carried out using transient plane source techniques with very small temperature perturbations of the sample material by the hot disk thermal constants analyzer. The transient plane source technique makes use of a thin sensor element in the shape of a double spiral. The hot disk sensor acts as both a heat source for generating temperature gradient in the sample and a resistance thermometer for recording the time-dependent temperature increase [15]. The encapsulated sensor was sandwiched between two pieces of samples. During a preset time, 200 resistance recordings were taken and from them a relation between temperature and time was established. The oxygen contents and valence state of manganese were determined using iodometric titration [16].

Table 1: Lattice parameters of the $Ca_{1-x}Gd_xMnO_{3-\delta}$ (0.00, 0.02, and 0.05).

Samples	a (Å)	b (Å)	c (Å)
$CaMnO_{3-\delta}$	5.27 (9)	7.43 (2)	5.26 (1)
$Ca_{0.98}Gd_{0.02}MnO_{3-\delta}$	5.24 (6)	7.44 (4)	5.28 (6)
$Ca_{0.98}Gd_{0.05}MnO_{3-\delta}$	5.26 (3)	7.43 (2)	5.28 (3)

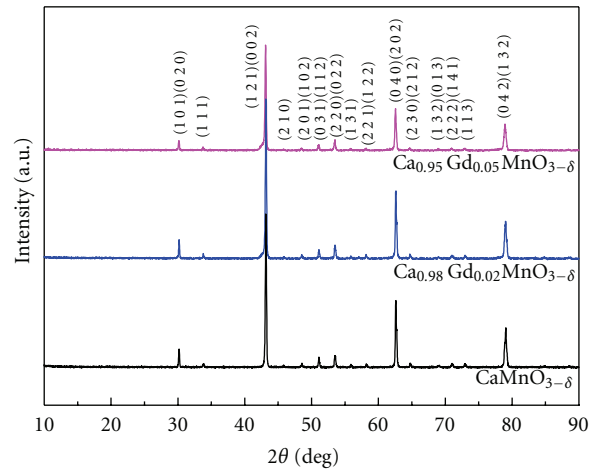

Figure 1: XRD patterns of the $Ca_{1-x}Gd_xMnO_{3-\delta}$ (0.00, 0.02, and 0.05).

3. Results and Discussion

XRD analysis indicates that all the samples of $Ca_{1-x}Gd_xMnO_{3-\delta}$ (0.00, 0.02, and 0.05) are a single phase with orthorhombic symmetry of *Pnma*. The typical XRD patterns are shown in Figure 1. The diffraction peaks are matched with earlier reports of $CaMnO_3$ [17], and no secondary phase is observed. The similarity between the crystal structures of undoped and doped samples suggests that the doped ions do not change the crystalline structure. Lattice parameters are calculated and tabulated in Table 1. As seen in Table 1, the lattice parameters do not show monotonic trend, which may be due to the oxygen deficiency and small amount of dopants. Trukhanov et al. [18] reported that lattice parameters changed due to the oxygen deficiency in $La_{0.50}Ca_{0.50}MnO_{3-\delta}$ ($0 \leq \delta \geq 0.50$). Wiebe et al. [19] also reported that lattice parameters changed due to the oxygen deficiency in $CaMnO_{3-\delta}$ ($\delta = 0.06, 0.11$).

Table 2 summarizes the characterization and properties of the samples at room temperature. The undoped sample shows the highest resistivity among the samples, while the resistivity of the doped samples is significantly lower than for the undoped sample due to the substitution of trivalent Gd^{3+} for divalent Ca^{2+}, which decreases the concentration of holes. The value of ρ for doped samples is in the range of 0.041 Ω–cm to 0.019 Ω–cm, which increases with increasing dopant content. For doped samples, the average valence of Mn^{v+} decreases and oxygen deficiency increases as compared to undoped sample. Doping of the Ca site with Gd causes a strong decrease of the ρ due to the creation of charge carrier content of Mn^{3+} in the Mn^{4+} matrix. The concentration of carriers in these samples can be correlated with the oxidation state of Mn. Creation of Mn^{3+} comes from two sources in the title system, that is, doping of Gd^{3+} and oxygen deficiency. Oxygen deficiency in $CaMnO_{3-\delta}$ creates two Mn^{3+} five-coordinate sites for each O vacancy according to the X-ray absorption near-edge spectra results [20]. In order to compensate the oxygen deficiency and maintain the electrical neutrality, the creation of Mn^{3+}could be present in these samples. There are also earlier reports, an oxygen deficiency for other electron-doped calcium manganites [21, 22]. The negative thermopower confirms that the dominant charge carriers are electrons for all the samples. The undoped $CaMnO_{3-\delta}$ has a very large absolute S, being about $-319\,\mu$V/K at 300 K. The room temperature absolute value of S for the undoped sample is lower than the value of $-600\,\mu$V/K reported by Flahaut et al. [23], which may be due to the oxygen deficiency. The doped samples show relatively small absolute S due to the increase of carrier concentration (Table 2). The doped sample induces a clear decrease of the absolute S value due to the increase of the concentration of Mn^{3+}.

The temperature dependence of resistivity of $Ca_{1-x}Gd_xMnO_{3-\delta}$ (0.00, 0.02, and 0.05) is shown in Figure 2. The undoped sample exhibit nonmetallic behavior in the entire temperature range, that is, the resistivity decreases with increasing temperature ($d\rho/dT < 0$). Similar tendency was also reported for undoped sample ($CaMnO_{3-\delta}$) [23]. The doped samples show that the resistivity increases with increasing temperature in the whole temperature range, indicating the metallic behavior ($d\rho/dT > 0$). This is a

Table 2: Room temperature characterization and properties of the $Ca_{1-x}Gd_xMnO_{3-\delta}$ (0.00, 0.02, and 0.05).

Samples	Mn^{v+}	δ	ρ (mΩ-cm)	S (μV/K)	κ_{total} (W/mK)	κ_{el} (W/mK)	κ_{ph} (W/mK)	PF (μW/cm K^2)	ZT
$CaMnO_{3-\delta}$	3.90 (8)	−0.04 (4)	102	−319	3.72	0.007	3.713	0.99	0.008
$Ca_{0.98}Gd_{0.02}MnO_{3-\delta}$	3.92 (8)	−0.02 (4)	041	−223	1.99	0.041	1.949	1.21	0.018
$Ca_{0.98}Gd_{0.05}MnO_{3-\delta}$	3.88 (9)	−0.03 (4)	019	−113	1.26	0.019	1.241	0.67	0.016

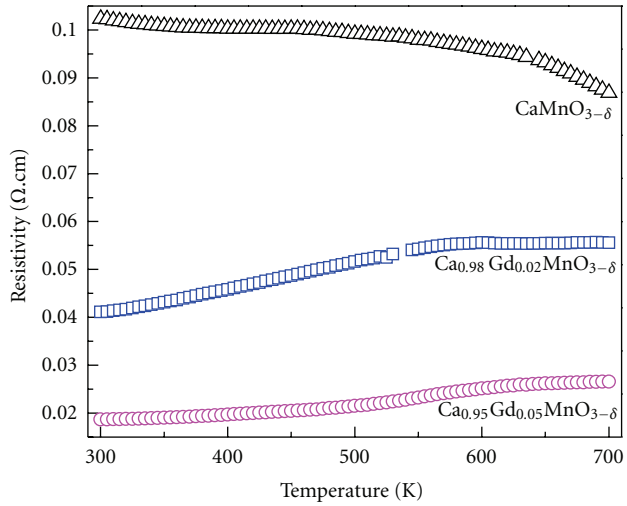

Figure 2: The temperature dependence of the electrical resistivity of the $Ca_{1-x}Gd_xMnO_{3-\delta}$ (0.00, 0.02, and 0.05).

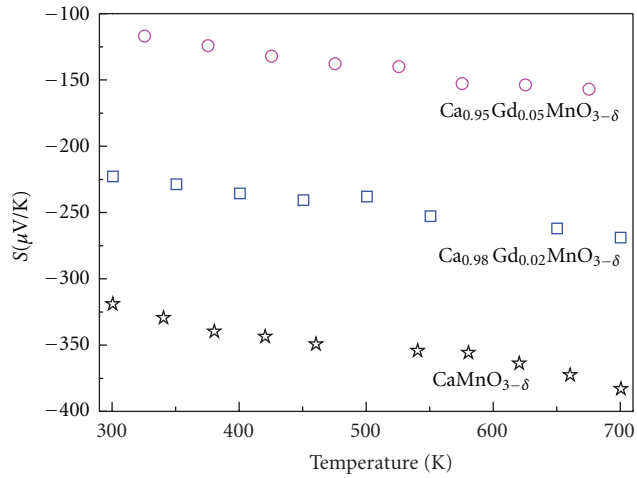

Figure 3: The temperature dependence of the Seebeck coefficient S of the $Ca_{1-x}Gd_xMnO_{3-\delta}$ (0.00, 0.02, and 0.05).

similar behavior to that of the electron-doped manganites above the metal-insulation transition temperature [24, 25].

Figure 3 shows the Seeback coefficient (S) as a function of temperature (300–700 K) for $Ca_{1-x}Gd_xMnO_{3-\delta}$ (0.00, 0.02, and 0.05). All samples exhibit negative values of the thermopower, which indicates that the electrons are the predominant charge carriers (n-type conduction). The absolute thermopower increases with increasing temperature and exhibit metallic behavior for undoped sample, which is contrast to Ohtaki's sample [26]. Ohtaki et al. [26] reported that absolute value of thermopower decreases with increasing temperature, typical characteristic of nonmetal-like temperature dependence. This difference should be attributed to the contribution of the oxygen deficiency [27].

For materials with more than one type of charge carrier, the diffusion thermopower can be expressed as

$$S = \sum_i \left(\frac{\sigma_i}{\sigma}\right) S_i, \tag{1}$$

where σ_i and S_i are the partial electrical conductivity and partial thermopower associated with the ith group of carriers, respectively. We can rewrite thermopower of $CaMnO_{3-\delta}$ and as

$$S = \frac{\sigma_{in}}{\sigma_{in} + \sigma_{ex,defect}} S_{in} + \frac{\sigma_{ex,defect}}{\sigma_{in} + \sigma_{ex,defect}} S_{ex,defect}, \tag{2}$$

where σ_{in} and S_{in} are the contribution from intrinsic carriers; $\sigma_{ex,defect}$ and $S_{ex,defect}$ are the contribution from extrinsic carriers due to oxygen defects. Since the increase of electrical conductivity ($\sim e^{-E_a/k_BT}$) is faster than the decrease of S ($\sim E_a/k_BT$) for semiconductors, one could expect that the second term in (2) would increase and therefore the absolute value of thermopower for $CaMnO_{3-\delta}$ would increase, which should be responsible for the simultaneous increase of the electrical conductivity and absolute value of thermopower with increasing temperature.

The experimental activation energies derived from electrical resistivity and thermopower measurements are distinguishable for the title system, and the adiabatic small polaron conduction model [28] has often been invoked to account for the transport mechanism in both electrical resistivity and thermopower [24, 26, 29]. Figure 4 shows similar fitting for $Ca_{1-x}Gd_xMnO_{3-\delta}$ (0.00, 0.02 and 0.05) in the present study using the following forms $\rho = \rho_0 T \exp(E_a/k_BT)$ and $S = (k_B/e)(W_H/k_BT + B)$, where E_a is one-half of the energy gap between the polaronic bands, W_H is one-half of the polaron binding energy, B is associated with the spin and the mixing entropy, and e is the electron charge with minus sign. One would expect a decrease of absolute value of thermopower with increasing temperature and obtain a negative W_H when fitting thermopower data for the polaronic transport.

The thermal conductivity is measured at room temperature, and values are presented in Table 2. Total thermal conductivity (κ_{total}) can be expressed as

$$\kappa_{total} = \kappa_{el} + \kappa_{ph}, \tag{3}$$

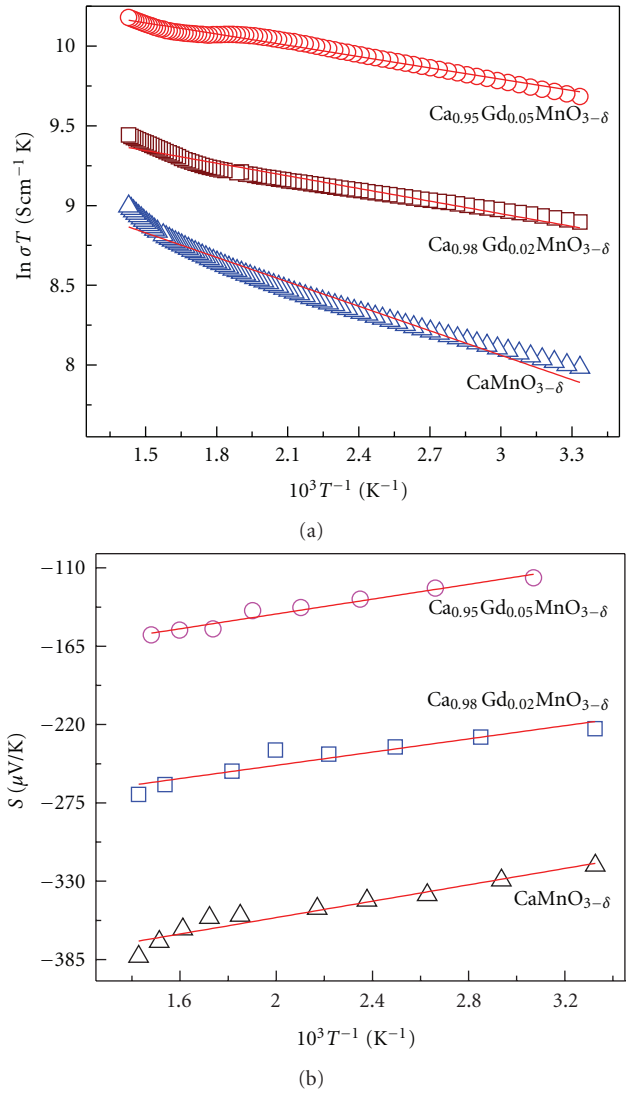

FIGURE 4: Plots of (a) In (σT) versus 1000/T and (b) S versus 1000/T of the $Ca_{1-x}Gd_xMnO_{3-\delta}$ (0.00, 0.02, and 0.05).

where κ_{el} and κ_{ph} represent the electronic and lattice thermal conductivity, respectively. κ_{el} can be calculated by using the Wiedemann-Franz-Lorenz relationship

$$\kappa_{el} = L\sigma T, \tag{4}$$

where $L = \pi^2k^2/3e^2 = 2.45 \times 10^{-8}\,\mathrm{W\,\Omega\,K^{-2}}$ is the Lorenz number and T is the absolute temperature. κ_{ph} is obtained by subtracting κ_{el} from κ_{total}. It can be clearly seen from Table 2 that the total thermal conductivity for all the doped samples is less than that of $CaMnO_{3-\delta}$. For materials with $\rho > 1\,\Omega$–cm, κ_{el} is negligible. But in our case, the resistivity is lower than 1 Ω–cm, a fact which leads us to determine the κ_{el} by using the Wiedemann-Franz law. The calculated value of κ_{el}, for $CaMnO_{3-\delta}$ is $0.019\,\mathrm{W\,m^{-1}\,K^{-1}}$ and $Ca_{0.95}Gd_{0.05}MnO_{3-\delta}$ is 0.027 at 700 K, respectively. For all the samples, the lattice contribution is more important than the electronic one. Due to the small κ_{el}, κ_{total} is mainly attributed to the lattice contribution. The κ_{total} of $Ca_{0.95}Gd_{0.05}MnO_{3-\delta}$ is 1.26 at 300 K, being an indication of these doping effects. It should be emphasized that in contrast to the $CaMnO_{3-\delta}$ and the $Ca_{0.95}Gd_{0.05}MnO_{3-\delta}$, samples show much lower κ_{total}. For all doped samples, the lattice contribution is more important than the electronic one. Due to the small κ_{el}, κ_{total} is mainly attributed to the lattice contribution. Both of the κ_{el}, κ_{ph} decrease with increasing dopant content (Table 2). The radius and mass of Gd^{3+} and Ca^{2+} ions are different, and substitution of Gd^{3+} and Ca^{2+} can affect the value of κ_{ph}. The effect of Gd^{3+} doping on the lattice vibration arises from two main factors. One is the crystallographic distortion and the other is the mass difference between Gd^{3+} and Ca^{2+} [24].

The power factor ($S^2\sigma$) is calculated and presented in Table 2. The highest value of $S^2\sigma$ ($1.21\,\mu\mathrm{W\,cm^{-1}\,K^{-2}}$ at 300 K) is obtained for $Ca_{0.98}Gd_{0.02}MnO_{3-\delta}$. The figure of merit ($ZT = S^2\sigma T/\kappa$) is calculated for all the samples. The calculated values are presented in Table 2. The highest ZT (0.018) is reached for $Ca_{0.98}Gd_{0.02}MnO_{3-\delta}$, which represents a 125% increase when compared to the $CaMnO_{3-\delta}$. Lan et al. [30] reported that the ZT value is ~0.02 at 300 K for $Ca_{0.94}Gd_{0.06}MnO_3$ prepared by the coprecipitation method and ZT value is ~0.018 at 300 K for $Ca_{0.96}Gd_{0.04}MnO_3$ prepared by solid state reaction, which is in agreement with our $Ca_{0.98}Gd_{0.02}MnO_{3-\delta}$ with $ZT = 0.018$ at 300 K. These results suggesting that there is scope for improvement of n-type materials for high-temperature thermoelectric application.

4. Conclusions

The thermoelectric properties (ρ, S, and κ) of $Ca_{1-x}Gd_xMnO_{3-\delta}$ ($x = 0.00$, 0.02, and 0.05) polycrystalline samples are investigated carefully. All the samples are a single phase with an orthorhombic structure. The iodometric titration results indicate that the electrical resistivity of $Ca_{1-x}Gd_xMnO_{3-\delta}$ correlates well with the average valence of the Mn^{v+} and oxygen deficiency. The smallest average valence of Mn^{v+} for $Ca_{0.95}Gd_{0.05}MnO_{3-\delta}$ has the smallest resistivity among the doped samples. The negative thermopower confirms that the domain carriers are electrons for all the samples. Doping of gadolinium on the calcium sites of $CaMnO_{3-\delta}$ produces reduction of resistivity and thermal conductivity. As a result, $Ca_{0.98}Gd_{0.02}MnO_{3-\delta}$ has the highest ZT among the doped samples. These results suggest that improving the thermoelectric properties is achived by doping concentration.

Acknowledgments

This work was supported by National Science Council (NSC) of Republic of China, Taiwan under the Grant no. NSC 98-2112-M-018-005-MY3. A. Bhaskar would like to express thanks to the postdoctoral fellowship sponsored NSC of Taiwan.

References

[1] I. Terasaki, Y. Sasago, and K. Uchinokura, "Large thermoelectric power in $NaCo_2O_4$ single crystals," *Physical Review B*, vol. 56, no. 20, pp. R12685–R12687, 1997.

[2] R. Funahashi, I. Matsubara, H. Ikuta, T. Takeuchi, U. Mizutani, and S. Sodeoka, "Oxide single crystal with high thermoelectric performance in air," *Japanese Journal of Applied Physics*, vol. 39, no. 11, pp. L1127–L1129, 2000.

[3] A. C. Masset, C. Michel, A. Maignan et al., "Misfit-layered cobaltite with an anisotropic giant magnetoresistance: $Ca_3Co_4O_9$," *Physical Review B*, vol. 62, no. 1, pp. 166–175, 2000.

[4] H. Leligny, D. Grebille, O. Pérez, A. C. Masset, M. Hervieu, and B. Raveau, "A five-dimensional structural investigation of the misfit layer compound $[Bi_{0.87}SrO_2]_2[CoO_2]_{1.82}$," *Acta Crystallographica Section B*, vol. 56, no. 2, pp. 173–182, 2000.

[5] H. Ohta, S. Kim, Y. Mune et al., "Giant thermoelectric Seebeck coefficient of a two-dimensional electron gas in $SrTiO_3$," *Nature Materials*, vol. 6, no. 2, pp. 129–134, 2007.

[6] A. Maignan, C. Martin, F. Damay, B. Raveau, and J. Hejtmanek, "Transition from a paramagnetic metallic to a cluster glass metallic state in electron-doped perovskite manganites," *Physical Review B*, vol. 58, no. 5, pp. 2758–2763, 1998.

[7] J. Hejtmanek, Z. Jirak, M. Marysko et al., "Interplay between transport, magnetic, and ordering phenomena in $Sm_{1-x}Ca_xMnO_3$," *Physical Review B*, vol. 60, no. 20, pp. 14057–14065, 1999.

[8] A. Urushibara, Y. Moritomo, T. Arima, A. Asamitsu, G. Kido, and Y. Tokura, "Insulator-metal transition and giant magnetoresistance in $La_{1-x}Sr_xMnO_3$," *Physical Review B*, vol. 51, no. 20, pp. 14103–14109, 1995.

[9] C. N. R. Rao, A. K. Cheetham, and R. Mahesh, "Giant magnetoresistance and related properties of rare-earth manganates and other oxide systems," *Chemistry of Materials*, vol. 8, no. 10, pp. 2421–2432, 1996.

[10] A. Maignan, C. Martin, F. Damay, and B. Raveau, "Factors governing the magnetoresistance properties of the electron-doped manganites $Ca_{1-x}A_xMnO_3$ (A = Ln, Th)," *Chemistry of Materials*, vol. 10, no. 4, pp. 950–954, 1998.

[11] K. Park and G. W. Lee, "Thermoelectric properties of $Ca_{0.8}Dy_{0.2}MnO_3$ synthesized by solution combustion process," *Nanoscale Research Letter*, vol. 6, no. 1, pp. 548–553, 2011.

[12] B. Fisher, L. Patlagan, G. M. Reisner, and A. Knizhnik, "Systematics in the thermopower of electron-doped layered manganites," *Physical Review B*, vol. 61, no. 1, pp. 470–475, 2000.

[13] G. D. Tang, C. P. Tang, X. N. Xu et al., "Electrical and thermal properties of the $Ca_{3-x}Gd_xCo_4O_{9+\delta}$ system," *Journal of Electronic Materials*, vol. 40, no. 5, pp. 504–507, 2011.

[14] C. J. Liu, "Structure and thermopower of solid solution nickelocuprates $La_{2-x}Sr_xCu_{1-y}Ni_yO_4$," *Philosophical Magazine B*, vol. 79, no. 8, pp. 1145–1159, 1999.

[15] C.-J. Liu, H.-C. Lai, Y.-L. Liu, and L.-R. Chen, "High thermoelectric figure-of-merit in p-type nanostructured $(Bi,Sb)_2Te_3$ fabricated via hydrothermal synthesis and evacuated-and-encapsulated sintering," *Journal of Materials Chemistry*, vol. 22, no. 11, pp. 4825–4831, 2012.

[16] C. J. Liu, M. D. Mays, D. O. Cowan, and M. G. Sánchez, "Composition-controlled metal-nonmetal transition in $La_{2-x}Sr_xNiO_{4-\delta}$," *Chemistry of Materials*, vol. 3, no. 3, pp. 495–500, 1991.

[17] K. R. Poeppelmeier, M. E. Leonowicz, J. C. Scanlon, J. M. Longo, and W. B. Yelon, "Structure determination of $CaMnO_3$ and $CaMnO_{2.5}$ by X-ray and neutron methods," *Journal of Solid State Chemistry*, vol. 45, no. 1, pp. 71–79, 1982.

[18] S. V. Trukhanov, N. V. Kasper, I. O. Troyanchuk, M. Tovar, H. Szymczak, and K. Bärner, "Evolution of magnetic state in the $La_{1-x}Ca_xMnO_{3-\delta}$ $(x = 0.30, 0.50)$ manganites depending on the oxygen content," *Journal of Solid State Chemistry*, vol. 169, no. 1, pp. 85–95, 2002.

[19] C. R. Wiebe, J. E. Greedan, J. S. Gardner, Z. Zeng, and M. Greenblatt, "Charge and magnetic ordering in the electron-doped magnetoresistive materials $CaMnO_{3-\delta}$ (δ=0.06,0.11)," *Physical Review B*, vol. 64, no. 6, Article ID 064421, pp. 644211–644217, 2001.

[20] Z. Zeng, M. Greenblatt, and M. Croft, "Large magnetoresistance in antiferromagnetic $CaMnO_{3-\delta}$," *Physical Review B*, vol. 59, no. 13, pp. 8784–8788, 1999.

[21] H. Taguchi and M. Shimada, "Metal-insulator transition in the system $(Ca_{1-x}La_x)MnO_{2.97}$ $(0.05 \leqq x \leqq 0.4)$," *Journal of Solid State Chemistry*, vol. 63, no. 2, pp. 290–294, 1986.

[22] H. Taguchi, M. Nagao, and M. Shimada, "Metal-insulator transition in the system $(Gd_{1-x}Ca_x)MnO_{2.98}$," *Journal of Solid State Chemistry*, vol. 82, no. 1, pp. 8–13, 1989.

[23] D. Flahaut, T. Mihara, R. Funahashi et al., "Thermoelectrical properties of A-site substituted $Ca_{1-x}Re_xMnO_3$ system," *Journal of Applied Physics*, vol. 100, no. 8, Article ID 084911, 4 pages, 2006.

[24] Y. Wang, Y. Sui, and W. Su, "High temperature thermoelectric characteristics of $Ca_{0.9}R_{0.1}MnO_3$ (R=La,Pr,Yb)," *Journal of Applied Physics*, vol. 104, no. 9, Article ID 093703, 7 pages, 2008.

[25] T. Kobayashi, H. Takizawa, T. Endo et al., "Metal-insulator transition and thermoelectric properties in the system $(R_{1-x}Ca_x)MnO_{3-\delta}$ (R: Tb, Ho, Y)," *Journal of Solid State Chemistry*, vol. 92, no. 1, pp. 116–129, 1991.

[26] M. Ohtaki, H. Koga, T. Tokunaga, K. Eguchi, and H. Arai, "Electrical Transport Properties and High-Temperature Thermoelectric Performance of $(Ca_{0.9}M_{0.1})MnO_3$ (M = Y, La, Ce, Sm, In, Sn, Sb, Pb, Bi)," *Journal of Solid State Chemistry*, vol. 120, no. 1, pp. 105–111, 1995.

[27] C. J. Liu, A. Bhaskar, and J. J. Yuan, "High-temperature transport properties of $Ca_{0.98}RE_{0.02}MnO_{3-\delta}$ (RE=Sm, Gd, and Dy)," *Applied Physics Letters*, vol. 98, no. 21, Article ID 214101, 2011.

[28] N. F. Mott and E. A. Davis, *Electronic Processes in Noncrystalline Materials*, Oxford University Press, Oxford, UK, 1979.

[29] C. J. Liu, C. S. Sheu, and M. S. Huang, "Nitrogen-annealing effects on the electrical resistivity and thermopower of layered $La_{1.4}Sr_{1.6}Mn_2O_{7+\delta}$ ceramics," *Physical Review B*, vol. 61, no. 21, pp. 14323–14326, 2000.

[30] J. Lan, Y. H. Lin, H. Fang et al., "High-temperature thermoelectric behaviors of fine-grained Gd-doped $CaMnO_3$ ceramics," *Journal of the American Ceramic Society*, vol. 93, no. 8, pp. 2121–2124, 2010.